PROCEEDINGS, Thirty-Sixth Workshop on Geothermal Reservoir Engineering
Stanford University, Stanford, California, January 31 - February 2, 2011
SGP-TR-191

3D TEMPERATURE MODEL OF THE HENGILL GEOTHERMAL AREA (ICELAND) REVEALED FROM ELECTROMAGNETIC DATA

Viacheslav V. Spichak, Olga K. Zakharova and Alexandra G. Goidina

Geoelectromagnetic Research Centre IPE RAS
Troitsk, Moscow Region, 142190, Russia
e-mail: v.spichak@mail.ru

ABSTRACT

Application of the modified indirect EM geothermometer based on the joint using of the available MT and TEM data enabled constructing of the deep three-dimensional temperature model of the Hengill geothermal area. The temperature accuracy estimations indicate that at the lower boundary of the model, corresponding to the depths around 20km, the average relative errors are equal to 26.5%.

The analysis of the temperature model has indicated that the lower boundary of the upper crust corresponding to the temperature of the brittle-to-ductile transition lies mainly at depths 15-20km. On the other hand, it is found that the solidus depth profile at the South Iceland Seismogenic Zone (SISZ) latitude agrees very well with the lower boundary of the EQ hypocenters, while the liquidus depth exceeds one determined from the linear extrapolation of the heat flow gradient measured in the boreholes. These findings mean that the crust in this area is more likely to be cool and thick than hot and thin.

Basing on the temperature model it is possible to guess that the extremely high temperatures estimated in the studied area originate from the molten liquid magma (with temperatures higher than basalt liquidus) upwelling from the mantle and accumulating in the shallow reservoir (magma chamber) located at the western margin of the studied area. Its further leakage in the upper crust look like two magma flows with the diameter around 3-5km: the northern arm is extending towards the Nesjavellir and the southern one – to the Hellisheidu and Hveragerdi fields.

The presence of a local heat source in the studied area explains the results of MT soundings, which have determined extremely well conducting layers at the depths corresponding to the locations of the high temperature intrusions. On the other hand, our results obtained for the Hengill geothermal area are in agreement with the hypothesis that shear wave attenuation in Icelandic crust is caused by local sources (in particular, by volcanoes) and is not diagnostic of the crust as a whole.

INTRODUCTION

The inferences on the internal structure of the unique Icelandic crust are based on the temperature estimations carried out either basing on the temperature measurements in the boreholes or by interpretation of the geophysical results in geothermal terms.

The temperature estimations in the earth crust are most naturally revealed from the heat flow gradient data (Hermance and Grillot, 1974; Flóvenz and Samundsson, 1993). However, a high dispersion of heat flow values in the mid-ocean ridge area does not enable accurate mapping of the crust temperature using routine interpolation / extrapolation techniques (Polyak et al., 1984).

The alternative way is based on using geophysical data including mainly magnetotelluric (MT) (Hermance, Grillot, 1974; Beblo, Bjornsson, 1978, 1980; Beblo et al., 1983; Hersir et al., 1984; Eysteinsson, Hermance, 1985; Flóvenz et al., 1985; Árnason et al., 2000; Bjornsson et al., 2005; Oskooi et al., 2005; Árnason et al., 2010, etc.) and seismic (Foulger et al., 1995; Menke et al., 1996; Tryggvason et al., 2002; Jousset et al., 2010, etc.) ones.

The temperature estimates has finally resulted in two alternative hypotheses on the crust structure. Some researchers (Beblo and Bjornsson, 1978, 1980; Bjornsson et al., 2005; Bjornsson, 2008, etc.) consider that the Icelandic crust is thin and hot (with the solidus temperatures reaching at depths 10-15km), while some others (Bjarnason et al., 1993; Menke et al., 1995, 1996; Menke and Sparks, 1995; Foulger et al., 2003, etc.) consider that it is thick and cold (the solidus temperature being reached at depths 20-30km).

These hypotheses are essentially based on the assessments of the brittle/ductile transition layer depth, which is characterized by the basalt solidus (around 650-700˚C). So, since the earthquakes occur

only in the brittle crust, the solidus isotherm should be beneath maximal depths of the EQ hypocenters (Foulger, 1995; Tryggvason et al., 2002; Bjornsson, 2008).

Another indicator of the mantle / crust transition zone is based on the detection in a number of places (though not everywhere) of the high conductivity layer of the thickness 3-5km in the depth range 10-20km (Beblo and Bjornsson, 1980; Beblo et al., 1983; Hersir et al., 1984; Bjornsson et al., 2005; Árnason et al., 2010). Finally, seismic velocity reduction, which was observed in some regions of Iceland (Tryggvason et al., 2002; Jousset et al., 2010), also characterize the depths, where the rock melting could occur.

Note that each of the above mentioned signs could be considered as necessary but not sufficient condition for the identification of the mantle / crust transition zone. In other words, none of them alone can assure correct estimation of the characteristic temperature depths and, correspondingly, serve as a basement for conclusions on the Icelandic crust type. It is worth mentioning in this connection that basing on the analysis of the seismic and magnetotelluric data Schmeling (1985) concluded that melting areas in the Icelandic crust better correlate with the models inferred from only electromagnetic (EM) than from only seismic data.

The reliability of the indirect temperature estimations by geophysical methods could be essentially increased by means of a joint analysis or inversion of the seismic and magnetotelluric data collected in the same area. Unfortunately, no such studies were carried out in the Hengill geothermal zone though 3D seismic velocity (Tryggvason et al., 2002; Jousset et al., 2010) and resistivity (Árnason et al., 2010) models were constructed up to the depth 10 km (with the exception of the demonstration of more deep resistivity cross-section in the latter paper).

Meanwhile, the methodology of the indirect EM temperature estimation (Spichak et al., 2010b) enables not only the temperature assessment much below the boreholes (Spichak and Zakharova, 2009a, b), but also constructing deep temperature cross-sections with relatively high accuracy (Spichak et al., 2010a). This study is aimed at building of the preliminary 3D temperature model of the Hengill geothermal area basing on the ground EM data and the available geotherms.

GEOLOGICAL SETTING

Iceland is very active tectonically as it is crossed by the Mid-Atlantic Ridge and its associated rift zones and transform faults. The Icelandic crust is mostly of volcanic origin with both intrusive and extrusive rocks (mainly oceanic-type flood basalts, tuffs, hyaloclastites and some acidic rocks) that were erupted under rift conditions. The abundant geothermal systems in Iceland are the results of volcanic activities and high heat flows. The high-temperature Hengill geothermal area located at south-west of the Iceland (Figure 1) is a triple junction where Reykjanes Volcanic Zone (RVZ), Western Volcanic Zone (WVZ) and the transform area (South Iceland Seismogenic Zone-SISZ) are intersected.

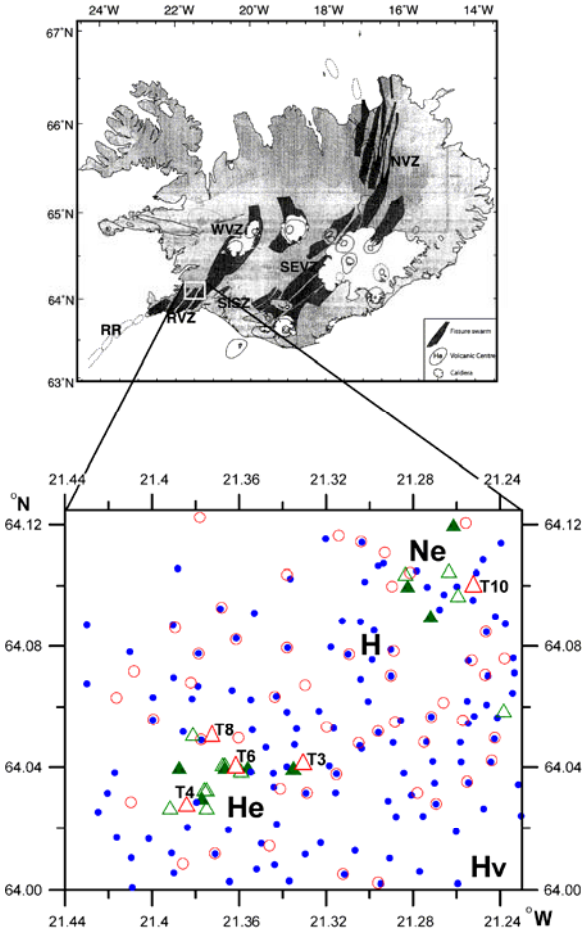

Figure 1: Map of the EM sites and boreholes. Red circles mark MT sites, blue dots mark TEM sites, triangles mark boreholes (green –boreholes used for calibration, red – boreholes used for EM geothermometer testing); H means Mt Hengill, He - Hellisheidi, Ne - Nesjavellir, Hv - Hveragerdi. Upper map is redrawn from (Tryggvason et al., 2002).

The Hengill volcanic complex hosts a huge geothermal system with an areal extend of about 100 km^2. The geothermal area is commonly divided into different, but connected sub-areas located in different directions from the Mt Hengill: the Hveragerdi area located at SE, the Nesjavellir area located at NE and the Hellisheidi area located at SW. The Hengill volcanic complex is very seismically

active with the seismicity and lateral movements mainly along faults and fractures associated with the transform tectonic pattern in the triple junction. The fault pattern revealed from the seismicity correlates well with the resistivity structure, showing that fluid flow in the geothermal system is highly controlled by tectonics.

Numerous deep geothermal wells have been drilled in the area, showing temperatures up to above 380°C with geothermal gradient ranging from 84±9˚C/km within the low-temperature geothermal area of the transform zone to 138±15˚C/km below the centre of the high-temperature geothermal area (Foulger, 1995).

EM DATA AND TEMPERATURE WELL LOGS

The EM data used for the temperature forecast consisted from MT and TEM sets (see Figure 1 for site locations). The former ones were collected in the Hengill area (in the framework of the INTAS project carried out in in 2005) by Phoenix equipment in the frequency range 5. 10^{-4} Hz with a remote station located 10 km away from the survey area. The distance between the MT sites and the ocean coast is sufficiently big at this frequency range, so the negative ocean effect on the further MT data interpretation could be neglected (see, for instance, Beblo et al., 1993). In order to fix the static shift problem we have used more than 100 1D resistivity profiles revealed from the central-loop transient electromagnetic (TEM) data by Occam's inversion (Árnason et al., 2010).

Calibration and testing of the indirect EM geothermometer required using the temperature well logs. They were selected from the deep boreholes distributed mainly in the high-temperature Hellisheidi and Nesjavellir fields so that the temperature records were dated wherever possible in the same period range as the EM measurements.

GENERAL SCHEME OF EM GEOTHERMOMETER APPLICATION

The application of the indirect EM geothermometer consists from the following general stages (Spichak et al., 2010b):

- measurement of the EM data at the surface;

- inversion of EM data resulting in the electrical conductivity/resistivity distribution in the earth;

- training of the artificial neural network (ANN) "with a teacher" by the correspondence between the electrical conductivity/resistivity profiles and the temperature logs from the adjacent wells;

- ANN temperature reconstruction in the point (profile, area, volume), where the conductivity/resistivity is determined.

In other words, the indirect EM temperature estimation is carried out by means of the artificial neural network calibrated by the correspondence between electrical conductivity/resistivity profiles revealed from EM data collected on the surface in the vicinity of available wells and appropriate temperature logs.

Taking into account the structure and locations of the EM and temperature data sets available in the Hengill geothermal area (see Figure 1) we have modified the above scheme as follows:

- first, the indirect EM geothermometer was created basing on the resistivity profiles revealed only from TEM data collected in the studied area (Árnason et al., 2010) and calibrated using the temperature records measured in the high-temperature wells;

- second, 3D resistivity model was reconstructed based on the TEM and MT data (similar to that obtained in the above mentioned paper); and,

- finally, 3D temperature model was determined in the same nodes of the spatial grid, where the resistiviy values were estimated.

CREATION OF THE INDIRECT EM GEOTHERMOMETER

In order to estimate the temperature values up to the depth 2 km the 1D resistivity profiles determined by the Occam's inversion of TEM data (Árnason et al., 2010) was used. To this end the ANN was taught (up to the misfit 6.6 %) by the correspondence between the resistivity values and spatial coordinates of the appropriate grid nodes. After this step the resulting ANN was used for estimating the resistivity values in the locations where the available 1489 temperature records were determined. Figure 2 shows corresponding Log resistivity and temperature profiles in the locations of 20 boreholes in Hellisheidi (a) and Nesjavellir (b) fields.

It is known (Árnason et al., 2000) that the temperature dependence of the alteration mineralogy makes it possible to interpret the resistivity distribution in terms of the temperature one provided that the temperature is in equilibrium with the dominant alteration. In order to ensure this condition ANN was learned by the correspondence between the spatial coordinates and the resistivity values, on the one hand, and the temperature values determined in the same nodes, on the other hand.

It is important to note that since the ANN input consisted not only from the electrical resistivity values but also from the corresponding node coordinates, the resistivity dependence on other local

factors (like geology, hydrology, alteration minerals, etc.) was implicitly taken into account, which, in turn, enabled more correct temperature forecast than that based on the laboratory study of the rock samples (Hermance and Grillot, 1974).

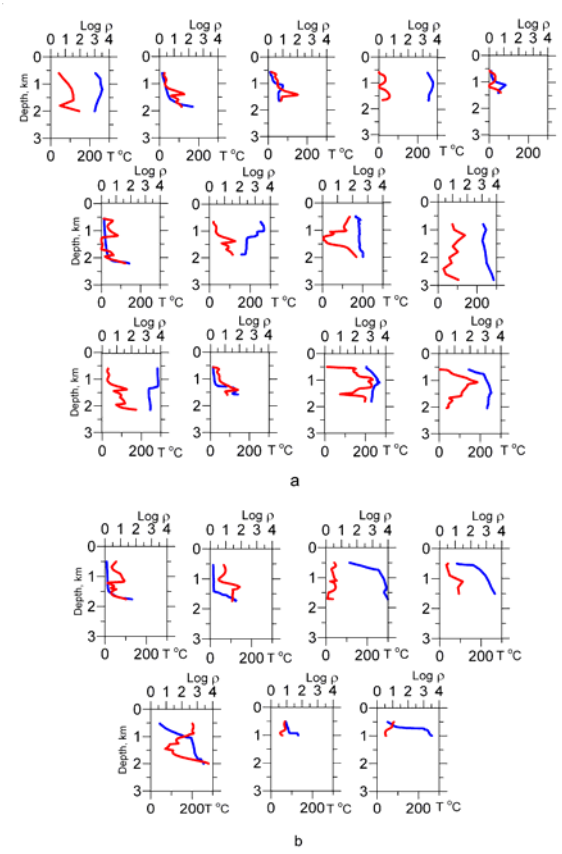

Figure 2: Temperature well logs (blue lines) and Log resistivity profiles (red lines) predicted by ANN taught by inverted MT and TEM data.

BUILDING OF 3D RESISTIVITY MODEL

The reconstruction of the temperature values in the nodes of a regular 3D grid by means of the indirect EM geothermometer requires prior electrical resistivity estimation in the pre-determined regular grid nodes. Taking into account that the resistivity structures revealed from full-range 3D and locally 1D inversion are similar (Árnason et al., 2010) we have restricted ourselves by using the latter approach.

In order to fix the static shift problem we have carried out a joint 3D ANN interpolation of the resistivity profiles revealed from MT and TEM data collected in the studied area (Figure 1). Accordingly, the teaching data pool for ANN consisted from all 1D resistivity profiles determined from TEM data (Árnason et al., 2010) up to the depth 1km and all 1D MT apparent resistivity determinant profiles starting from this depth. In contrary to the traditional approach to the static shift correction using the TEM data collected in the same locations as MT data (see, for instance, the above paper) our approach enables using all MT and TEM data measured in the studied area, which, in turn, improves the accuracy, especially when the MT and TEM data are measured in different locations.

The ANN was taught then by the correspondence of the spatial coordinates, on the one hand, and the resistivity values, on the other hand. After ANN teaching it was used for the resistivity estimation in the nodes of 3D regular grid with spacing 0.004˚ (latitude) x 0.005˚ (longitude) x 2.5 km (depth).

TESTING OF THE INDIRECT EM GEOTHERMOMETER

Before the temperature forecasting by the resistivity values determined at the previous stage we have tested the accuracy of the temperature extrapolation in depth using the temperature well logs measured in 5 high-temperature deep boreholes not used for the EM geothermometer calibration (see Figure 1 for appropriate wells location). To this end appropriate artificial neuronets were trained in correspondence between the temperature values and electrical resistivity estimated from MT and TEM data at a neighboring sites.

The whole depth of each well was divided into 10 intervals and the training was carried out successively at 1/10, 2/10, 3/10, ... fractions of the depth. After the training the neuronets were tested at the remaining parts of temperature profiles the data from which have not been employed for training. Following the inference of the paper (Spichak and Zakharova, 2009b) we did not used for calibration the data from the upper 0.5 km of each resistivity and temperature profile so that to avoid the negative affects of the topography as well as of the near-surface geological and hydrological heterogeneities.

Shown in Table 1 are the errors of well temperature estimation at different depths depending on what portion δ of temperature and electrical resistivity profiles (from the surface to maximal well depths) have been used for calibration. It can be seen from the Table 1 that for all wells the testing errors ε decrease with increasing δ (on average, from 26.5% at $\delta = 0.1$ to 2.7% at $\delta = 0.9$). Yet starting from $\delta = 0.3$ the errors ε of extrapolation in depth become, on average, lower than 10% although this level for different wells is arrived at different values of δ.

In Figure 3 a plot is shown illustrating the dependence of the mean relative error ε of the neuronet extrapolation of temperature in depth (based on electromagnetic data measured at the site closest

to the well versus the portion of the profiles used for the neuronet training.

Table 1: Temperature prognosis errors (in per cent) for 5 boreholes and adjacent MT sites depending on the portion δ of the resistivity and temperature profiles used for calibration

.

δ	T10-MT81	T3-MT44	T4-MT38	T6-MT49	T8-MT53
0.1	45.5	20.1	27.0	17.0	22.7
0.2	16.6	6.5	14.0	3.4	28.3
0.3	4.9	8.7	15.2	3.6	10.2
0.4	2.0	7.6	2.5	2.1	4.0
0.5	1.0	7.5	2.6	1.6	2.8
0.6	3.4	2.7	3.0	1.5	4.3
0.7	0.9	2.5	2.4	2.8	5.2
0.8	0.6	3.0	5.1	0.5	3.6
0.9	0.2	2.7	4.7	1.2	4.7

From this plot one can conclude that extrapolation to the depths, say, twice as large as the borehole lengths results in errors ranging from 0.9% to 5.3%, while extrapolation to the depths 9 times bigger than the well depth results in the errors ranging from 15.4% to 36.6%. Assuming that the accuracy estimates obtained in testing of the geothermometer in the depth range 0-2 km remain valid also in a bigger depth scale we could assess the potential relative temperature errors using the graph and appropriate bars in a Figure 3.

BUIILDING OF 3D TEMPERATURE MODEL

The temperature values for the studied area from the depth 0.5 km up to the depth 20 km were reconstructed by the indirect EM geothermometer in the same nodes of the spatial grid, in which the resistivity values were determined above. It is worth mentioning in this connection that despite the resistivity is determined up to the depth 100 km, the temperature reconstruction is demonstrated here only up to the depth 20 km, where the relative errors according to the testing results (Figure 3) are ranging from 15.4% to 36.6%.

Figures 4-5 demonstrate horizontal and vertical temperature cross-sections at different depths and longitudes, accordingly. Figure 6 shows the isosurfaces of the basalt solidus (T=650˚C) and liquidus (T=1120˚C), while the Figure 7 compares the temperature cross-section and the EQ hypocenters' locations at the same profile.

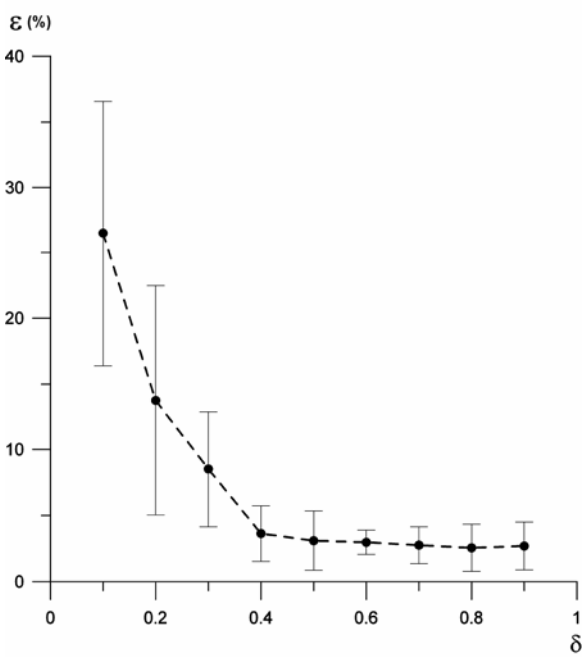

Figure 3: Dependence of the average relative error ε (in per cent) of the EM temperature extrapolation on the portion δ of the temperature well logs and electrical resistivity profiles used for the neuronet training.

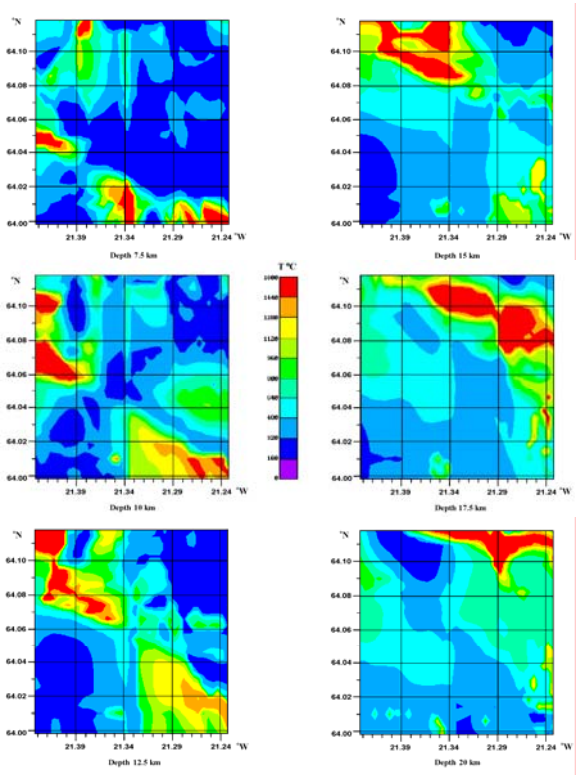

Figure 4: Slices of the temperature distribution at different depths.

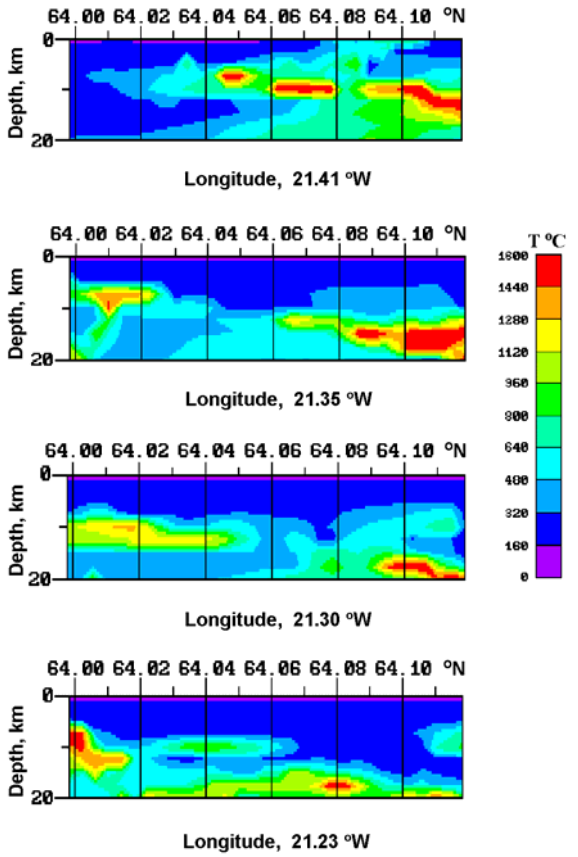

Figure 5: Temperature cross-sections at different longitudes.

RESULTS

The main results of the temperature model analysis are as follows.

1. The temperature distribution in the studied area, being essentially laterally inhomogeneous up to the depth 15km, is becoming rather homogeneous at larger depths (Figure 4). As this takes place, the temperature up to the depth 20km is mainly sub-solidus (Figure 6a).

2. A shallow high temperature anomaly (with temperature higher than 1400˚C) localized at the depths 2-3 km between the latitudes 64.08˚N и 64.10˚N at the western margin of the studied area (longitude 21.43˚ W) is detected (Figures 4 and 5). It extends in the crust along two arms: towards NE (in the direction of Nesjavellir) and towards SE (in the direction of Hellisheidi and Hveraverdi). The link between the latter geothermal fields is well seen also from the spatial locations of the solidus isotherm (Figure 6a) and especially of the liquidus isotherm (Figure 6b).

3. Basing on the horizontal temperature slices (Figure 4) it is possible to pick out the horizontal temperature jumps: (1) extending in the SN direction at the longitude 21.33˚W up to the depth 12.5km and (2) diagonal one extending in the SW-NE direction at depths 8-10 km. They reflect the general seismicity distribution in the area based on the regional transform tectonic lineaments (see (Árnason et al., 2010) and references therein).

4. The northern arm of the high temperature channel falls down from the depths 2-3 km at the heat source up to the depths 20-22km at the NE of the studied area (to the north from Nesjavellir) (Figure 4). Its roof (with temperatures reaching 640 ˚C) is located in the Nesjavellir field at the depth 7.5km, which is consistent with the depth of the well conducting layer detected there by magnetotelluric sounding (Hersir et al., 1984).

5. A small-scale temperature anomaly is located at the depth 15km beneath the Mt Hengill. It has a horizontal diameter 2.5-3km and maximal temperature reaching the solidus (Figure 4). It is connected with the extensive and even more hot area located at depths 15-20km beneath the Nesjavellir field (Figure 5, slice along the longitude 21.3 ˚W).

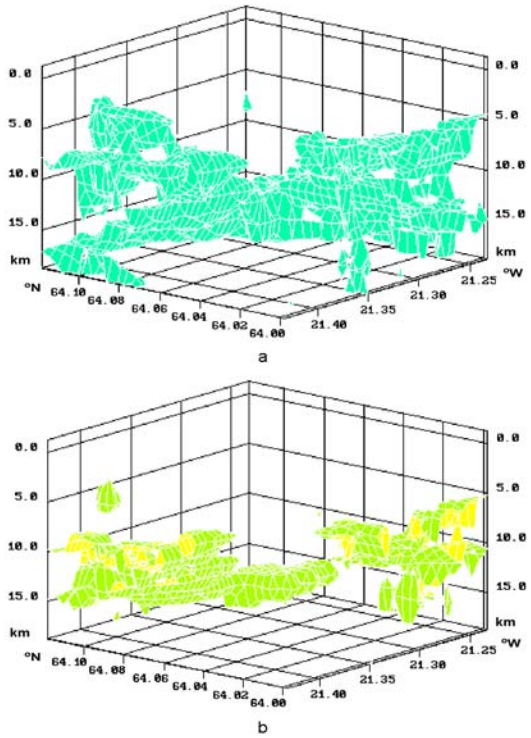

Figure 6: Isosurfaces of temperatures T = 640 ˚C (a) and T = 1120 ˚C (b).

6. Along the southern arm the high temperature magma flow extends from the heat source towards SE in the direction of Hellisheidi and Hveragerdi. In the Hellisheidi it is traced at depths 5-10km, while in the Hveragerdi it goes down up to the depths 7.5-12.5km (Figures 4 and 5). The link between these high temperature anomalies is well seen also from the

spatial location of the above mentioned isosurfaces (Figure 6a,b).

7. The comparison of spatial locations of the solidus and liquidus isosurfaces (Figure 6a,b) indicates: (1) unlike the former isosurface covering practically the whole studied area and located in the depth range 15-20km the latter one is traced only along the northern and southern arms of the high temperature magma flow; (2) the vertical distance between these isosurfaces (where both of them are determined) is mainly about 1-2km.

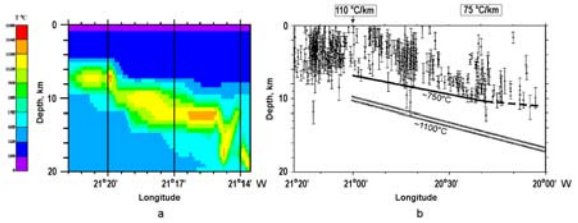

Figure 7: (a) Temperature cross-section at latitude 64˚ 1' N ; (b) SISZ: correlation between maximum depth of earthquakes (single line), depth to the conductive layer with partial melt (double line) and surface temperature gradient (after Bjornsson, 2008).

8. As it is seen from the temperature cross-section along the latitude 64˚1' (Figure 7a) corresponding to the location of SISZ, the high temperature channel is slowly deepening away from the shallow heat source located at the western margin of the studied area. Its upper boundary (T>640˚ C) is shifted from the depths 5-6km at the West to 10-11km at the East (which is consistent with the estimates made in (Foulger, 1995; Tryggvason et al., 2002; Bjornsson, 2008) and even in details follows the lower boundary of the EQ hypocenters (compare the fragments of the Figures 7a and 7b between 21˚14'W and 21˚20'W). Meanwhile, the isotherm T=1120˚ C is detected, as it is seen from the Figure 7a, at the depth 7km at the western end of the profile and approximately at the depth 14km at its eastern end, which is noticeably deeper than the depths forecasted by Bjornsson (2008) basing on the linear extrapolation of the heat flow gradient measured in the boreholes (Figure 7b).

CONCLUSIONS

Application of the indirect EM geothermometer based on the joint using of the available MT and TEM data enabled constructing of the deep three-dimensional temperature model of the geothermal area. The temperature accuracy estimations indicate that at the lower boundary of the model, corresponding to the depths around 20km, the average relative errors are equal to 26.5%.

The analysis of the temperature distribution in the Hengill geothermal area has indicated that the lower boundary of the upper crust corresponding to the temperature of the brittle-to-ductile transition lies mainly at depths 15-20km. On the other hand, the solidus depth profile at the SISZ latitude agrees very well with the lower boundary of the EQ hypocenters, while the liquidus depth exceeds one determined from the linear extrapolation of the heat flow gradient measured in the boreholes. These results support the hypothesis on the cool and thick Icelandic crust proposed in (Bjarnason et al., 1993; Menke and Sparks, 1995; Menke et al., 1996; Foulger et al., 2003).

Basing on the temperature model it is possible to guess that the high temperatures in the studied area originate from the molten liquid magma (with temperature higher than liquidus) upwelling from the mantle and accumulating in the shallow reservoir (magma chamber) located at the western margin of the studied area. Its further leakage in the upper crust is going along two main channels with the diameter around 3-5km: the northern arm is extended towards the Nesjavellir and the southern one is moving towards the Hellisheidu and Hveragerdi.

The presence of a local heat source in the studied area explains the results of MT soundings (Árnason et al., 2010; etc.), which have determined extremely well conducting layers at the depths corresponding to the locations of the high temperature channels (it is worth mentioning in this connection that Eysteinsson and Hermance (1985) attributed the high electrical conductivity of the detected layer to the temperatures up to 1300˚C). Similar anomalies found in other areas of Iceland, might also have a localized source and not be indicative of the whole crust. On the other hand, our results obtained for the Hengill geothermal area are in agreement with the hypothesis of Menke et al. (1996) that shear wave attenuation in Icelandic crust is caused by local sources (in particular, by volcanoes) and is not diagnostic of the crust as a whole. This hypothesis is also consistent with the results of modeling (Schmeling and Marquart, 2008).

In conclusion it is worth mentioning that in order to increase the reliability of the inferences regarding the Icelandic crust basing on the geophysical data it is important to provide a joint 3D analysis / inversion of the EM and seismic data as well as temperature well logs collected in the same area. Any attempts to draw conclusions on the Icelandic crust basing on different geophysical data sets collected at different time intervals and/or in different parts of Iceland may require highly sophisticated hypotheses for their interpretation, which could be far from the reality.

ACKNOWLEDGMENTS

The authors acknowledge Drs. H. Eysteinsson and K. Árnason who kindly offered the TEM data collected in the Hengill area and Reykjavik Energy, Inc. who

offered the temperature well logs. This work was supported by the INTAS (project no. 03-51-3327) and the Russian Foundation for Basic Research (project no. 11-05-00045).

REFERENCES

Árnason, K., Eysteinsson, H., and Hersir, G.P. (2010), "Joint 1D inversion of TEM and MT data and 3D inversion of MT data in the Hengill area, SW Iceland", *Geothermics*, **39**, 13-34.

Árnason, K., Karlsdottir, R., Eysteinsson, H., Flóvenz, O. G., Gudlaugsson, S. T. (2000), "The resistivity structure of high-temperature systems in Iceland", *Proc. World Geothermal Congress*, Kyushu-Tohoku, Japan, 923-928.

Beblo, M., Bjornsson, A. (1978), "Magnetotelluric investigation of the lower crust and upper mantle beneath Iceland", *J. Geophys.*, **45**, 1-16.

Beblo, M., Bjornsson, A. (1980), "A model of electrical resistivity beneath NE-Iceland, correlation with temperature", *J. Geophys*., **47**, 184-190.

Beblo, M., Bjornsson, A., Árnason, K., Stein, B., Wolfgram, P. (1983), "Electrical conductivity beneath Iceland - constraints imposed by magnetotelluric results on temperature, partial melt, crust and mantle structure", *J. Geophys*., **53**, 16-23.

Bjarnason, I.Th., Menke, W., Flovenz, O.G., and Caress, D. (1993). "Tomographic image of the Mid-Atlantic plate boundary in south western Iceland", *J. Geophys. Res.*, **98**, 6607-6622

Bjornsson, A. (2008), "Temperature of the Icelandic crust: Inferred from electrical conductivity, temperature surface gradient, and maximum depth of earthquakes", *Tectonophysics*, **447**, 136-141.

Bjornsson, A., Eysteinsson, H., and Beblo, M. (2005), "Crustal formation and magma genesis beneath Iceland: magnetotelluric constraints". In: *Geological Society of America Special Paper*, **388**, 665-686.

Eysteinsson, H. and Hermance, J.F. (1985), "Magnetotelluric measurements across the eastern neovolcanic zone in South Iceland", *J. Geophys. Res*., **90**, B12, 10,093-10,103.

Flóvenz, O.G. and Samundsson, K. (1993), "Heat flow and geothermal processes in Iceland", *Tectonophysics*, **225**, 123-138.

Flóvenz, O.G., Georgsson, L.S., and Arnason, K. (1985), "Resistivity Structure of the Upper Crust in Iceland", *J. Geoph. Res*., **90**, B12, 10136-10150.

Foulger, G.R. (1995), "The Hengill geothermal area, Iceland: variation of temperature gradients deduced from the maximum depth of seismogenesis", *J. Volc. Geoth. Res*., **65**, 119-133.

Foulger, G.R., Du, Z., Julian, B.R. (2003), "Icelandic-type crust", *Geophys. J. Intern.*, **155**, 567-590.

Foulger, G.R., Miller, A.D., Julian, B.R., and Evance, J.R. (1995). "Three-dimensional Vp and Vp/Vs structure of the Hengill triple junction and geothermal area, Iceland, and the repeatability of tomographic inversion", *Geophys. Res. Lett.*, **22**, 1309-1312.

Hermance, J.F. and Grillot, L.R. (1974), "Constraints on temperatures beneath Iceland from magnetotelluric data", *Phys.Earth Planet. Int*., **8**, 1-12

Hersir, G.P., Bjornsson, A., Pedersen, L.B. (1984), "Magnetotelluric survey across the active spreading zone in southwest Iceland", *J. Volc. Geoth. Res*., **20**, 253-265.

Jousset, P., Haberland, C, Bauer, K., Árnason, K. (2010), "Detailed structure of the Hengill geothermal volcanic complex, Iceland, inferred from 3-D tomography of high-dynamic broadband seismological data", *Proc. World Geothermal Congress*, Bali, Indonesia.

Menke, W., Brandsdottir, B., Einarsson, P. and Bjarnason, I.T. (1996), "Reinterpretation of the RRISP-77 Iceland shear-wave profiles", *Geophys. J. Int.*, **126**,166-172.

Menke, W. and Sparks, D. (1995), "Crustal accretion model for Iceland predicts cold crust", *Geophys. Res. Lett.*, **22**, 1673-1676.

Oskooi, B., Pedersen, L. B., Smirnov, M., Árnason, K., Eysteinsson, H. and Manzella, A. (2005), "The deep geothermal structure of the Mid-Atlantic Ridge deduced from MT data in SW Iceland". *Phys.Earth Planet. Int*., **150**, 183–195.

Polyak, B.G., Kononov, V.I., and Khutorskoy, M.D. (1984), "Heat Flow and Structure of the Lithosphere of Iceland in Light of New Data", *Geotectonics*, **18** (1), 79-85.

Schmeling, H. (1985), "Partial melt below Iceland: a combined interpretation of seismic and conductivity data", *J. Geophys. Res.*, **90**, BI2, 10,105-10,116.

Schmeling, H. and Marquart, G. (2008), "Crustal accretion and dynamic feedback on mantle melting of a ridge centred plume: the Iceland case", *Tectonophysics*, **447**, 31 - 52

Spichak, V., Borisova, V., Fainberg, E., Khalezov, A. and Goidina, A. (2007), "Electromagnetic 3D tomography of the Elbrus volcanic center according to magnetotelluric and satellite data", *J. Volc. Seism.,* **1,** 53-66.

Spichak, V., Geiermann, J., Zakharova, O., Calcagno, P., Genter, A. and Schill, E. (2010a), "Deep temperature extrapolation in the Soultz-sous-Forêts geothermal area using magnetotelluric data". Expanded Abstr. *XXXV Workshop on Geothermal Reservoir Engineering Stanford University*, Stanford, California.

Spichak, V. and Zakharova, O. (2009a), "Electromagnetic temperature extrapolation in depth in the Hengill geothermal area, Iceland". Expanded Abstr. *XXXIV Workshop on Geothermal Reservoir Engineering*, Stanford University, Stanford, USA.

Spichak, V. and Zakharova, O. (2009b), "The application of an indirect electromagnetic geothermometer to temperature extrapolation in depth", *Geophysical Prospecting*, **57**, 653-664.

Spichak, V., Zakharova, O. and Rybin, A. (2010b), "Methodology of the indirect temperature estimation basing on magnetotelluruc data: northern Tien Shan case study", *J. Appl. Geoph.*, doi: 10.1016/j.jappgeo.2010.12.007.

Tryggvason, A., Rognvaldsson, S.Th.. Flovenz, O.G. (2002), "Three-dimensional imaging of P- and S-wave velocity structure and earthquake locations beneath Southwest Iceland", *Geophys. J. Int*. **151**, 848-866.